IEEE Access
Multidisciplinary : Rapid Review : Open Access Journal

Received August 17, 2021, accepted September 6, 2021, date of publication September 9, 2021, date of current version September 17, 2021.

Digital Object Identifier 10.1109/ACCESS.2021.3111439

A High Torque Estimation Accuracy Direct Torque Control of Permanent Magnet Synchronous Motor Based on a Novel Iron Loss Resistance Observer

ZHEN JIN[1], JIANFEI YANG[1,2], XIN QIU[1,2], HAORUI GE[1], (Graduate Student Member, IEEE), AND CHENGUANG BAI[1]

[1]School of Electrical and Automation Engineering, Nanjing Normal University, Nanjing 210046, China
[2]Jiangsu Key Laboratory of 3D Printing Equipment and Manufacturing, Nanjing 210042, China

Corresponding author: Jianfei Yang (631056602@qq.com)

This work was supported in part by the National Nature Science Foundation of China under Project 51407095, Project 51607094, and Project 51907027; in part by the Natural Science Foundation of Jiangsu Province under Project BK20151548; in part by the Six Talent Peaks Project in Jiangsu Province under Project GDZB-043; and in part by the Science and Technology Achievement Transformation Project of Jiangsu Province under Project BA2018035.

ABSTRACT This paper proposes a direct torque control (DTC) of permanent magnet synchronous motor (PMSM) with high torque estimation accuracy. Based on the PMSM mathematical model considering iron loss resistance, this paper analyzes that when using stator current to estimate torque, the accuracy will be affected by iron loss resistance. Using stator magnetizing current can solve the current deviation caused by iron loss resistance and improve torque estimation accuracy. Since the stator magnetizing current cannot be obtained directly, a novel iron loss resistance observer based on the model reference adaptive system (MRAS) is designed to estimate iron loss resistance and stator magnetizing current simultaneously. Popov's hyperstability theory guarantees the stability of the designed observer. Finally, a 1kW PMSM experimental platform is constructed to verify the proposed method. Both the simulation and experimental results show that the designed observer is stable, and using stator magnetizing current to estimate torque has better accuracy than stator current.

INDEX TERMS Permanent magnet synchronous motor, direct torque control, model reference adaptive system, iron loss resistance, stator magnetizing current.

I. INTRODUCTION

Permanent magnet synchronous motor(PMSM) has many advantages, such as simple structure, reliable operation, low loss, high efficiency, flexible size, which is widely used in electric vehicle drive systems [1], [2]. Electric vehicles usually work in torque control mode, and the controller's command is the torque reference value. The torque control accuracy is crucial to the safe driving of vehicles because the power distribution has a significant dependence on the torque accuracy [3]. Installing a high-accuracy torque sensor will lead to higher costs and lower vehicle reliability. Therefore, it is necessary to study a high-performance control strategy to improve torque control accuracy.

The high-performance motor control strategies, including direct torque control (DTC) and field-oriented control (FOC), have been widely applied to PMSM drive systems [4]. Compared with FOC, DTC has no current regulator, insensitivity to motor parameters, and fast dynamic response in torque control [6], which has been widely used in various applications since its successful implementation on the PMSM in the late 1990s [7]. The control variables in DTC are stator flux linkage and electromagnetic torque, and the estimation accuracy of the feedback loop directly determines the control performance. Generally speaking, the stator flux linkage is estimated by integrating its back electromotive force (BEMF), and the electromagnetic torque is estimated by cross-product of stator flux linkage and stator current [7]–[9].

The method of integrating BEMF to estimate stator flux linkage is susceptible to parameter mismatch, cumulative error of integrator, inverter dead-time effects. Many scholars have carried out a lot of research to improve the estimation accuracy of stator flux linkage. Theoretically, the only motor

The associate editor coordinating the review of this manuscript and approving it for publication was Zhuang Xu.

parameter that affects the estimation of stator flux linkage is stator resistance R_s. A novel stator resistance estimator based on the model reference adaptive system (MRAS) is studied [10]. As for the cumulative error caused by the integral calculation, the improved low-pass filter with error compensation [11] and several closed-loop stator flux linkage observers were proposed to improve the estimation accuracy [12], [13]. In addition, since the BEMF is not easy to measure directly, the commanded voltage vector is used to estimate the stator flux linkage. The error between the actual voltage vector and the commanded voltage vector caused by the dead time effect reduces the estimation accuracy. Several approaches have solved this problem through current polarity detection or designing disturbance observers [14]–[16].

The above research has effectively improved the estimation accuracy of stator flux linkage. Based on the simplified PMSM mathematical model, the estimation of torque depends on stator flux linkage and stator current. However, the simplified model only considers copper loss and ignores iron loss. To further improve the control performance, a more accurate mathematical model should be used. Many scholars have carried out a lot of research on the mathematical model of PMSM considering iron loss. [17] established a speed sensorless system based on the mathematical model considering iron loss, which improved speed estimation accuracy and load range at low speed. [18] improved the minimization loss control based on the iron loss model, which comprehensively reduces electrical loss of the IPMSM. The above research based on the PMSM mathematical model considering iron loss has achieved better performance [17], [18]. According to the iron loss model, the stator current includes two parts: stator magnetizing current and stator iron loss current. [17]–[21] described that the stator magnetizing current should be used to calculate the torque. However, the stator magnetizing current cannot be effectively obtained in the application; only the stator current can be calculated through coordinate transformation. Therefore, it is meaningful to study how to estimate stator magnetizing current and improve the torque estimation accuracy.

This paper aims to improve the torque estimation accuracy in DTC by using stator magnetizing current instead of stator current. Firstly, based on the mathematical model considering iron loss resistance, it is analyzed that using stator magnetizing current to estimate torque can avoid the estimation error caused by iron loss resistance. However, the stator magnetizing current cannot be measured or calculated directly; only the stator current can be measured by the sensor and calculated through coordinate transformation. Therefore, a novel iron loss resistance observer based on the MRAS is designed to estimate iron loss resistance and stator magnetizing current simultaneously. The adaptation law is derived from the Popov hyperstability theory. Finally, the simulation and experimental results show that the designed observer performs well in estimating the iron loss resistance and stator magnetizing current, and the torque estimation accuracy can be improved by using the estimated magnetizing current.

II. MATHEMATICAL MODEL OF PMSM CONSIDERING IRON LOSS RESISTANCE

In the rotating coordinate system, the mathematical model of PMSM considering iron loss resistance [20] is shown in Fig. 1.

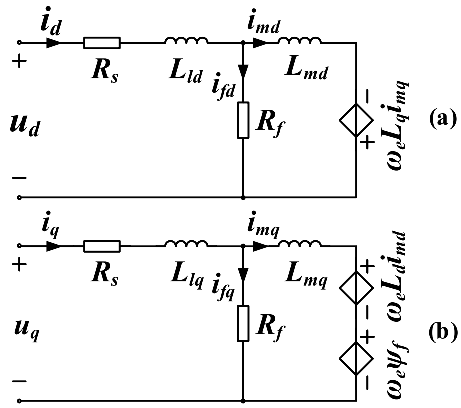

FIGURE 1. Equivalent circuit of PMSM considering iron loss. (a) Equivalent circuit of d-axis. (b) Equivalent circuit of q-axis.

Based on Fig. 1, the voltage equations of the PMSM considering iron loss are expressed as:

$$\begin{cases} L_{ld}\dfrac{di_d}{dt} = -\left(R_s + R_f\right) i_d + R_f i_{md} + u_d \\ L_{lq}\dfrac{di_q}{dt} = -\left(R_s + R_f\right) i_q + R_f i_{mq} + u_q \\ L_{md}\dfrac{di_{md}}{dt} = R_f\left(i_d - i_{md}\right) + w_e L_q i_{mq} \\ L_{mq}\dfrac{di_{mq}}{dt} = R_f\left(i_q - i_{mq}\right) - w_e L_d i_{md} - w_e \psi_f \end{cases} \tag{1}$$

In equation(1), u_d and u_q are d-axis and q-axis voltages; i_d and i_q are d-axis and q-axis stator current; i_{md} and i_{mq} are d-axis and q-axis stator magnetizing current; i_{fd} and i_{fq} are d-axis and q-axis stator iron loss current; R_s and R_f are stator resistance and iron loss resistance; L_d and L_q are d-axis and q-axis inductances; L_{md} and L_{mq} are d-axis and q-axis magnetizing inductance; L_{ld} and L_{lq} are d-axis and q-axis leakage inductance; ω_e is the rotor electric angular speed; ψ_f is the rotor flux linkage.

The stator flux linkage and torque equations of the PMSM considering iron loss are given as follows [21]:

$$\begin{cases} \psi_d = L_{md} i_{dm} + \psi_f \\ \psi_q = L_{mq} i_{qm} \\ T_e = \dfrac{3}{2} P_n \left(\boldsymbol{\psi}_s \otimes \boldsymbol{i}_{sm}\right) \\ \quad = \dfrac{3}{2} P_n \left(\psi_d i_{mq} - \psi_q i_{md}\right) \end{cases} \tag{2}$$

where T_e is the electromagnetic torque; P_n is the pole-pair numbers; $\boldsymbol{\psi}_s$ is the stator flux linkage vector; $\boldsymbol{i}_{sm}$ is the stator magnetizing current vector; ψ_d and ψ_q are d-axis and q-axis stator flux linkage; and $\otimes$ represents cross product.

According to equation(2), it is necessary to obtain ψ_d, ψ_q and i_{md}, i_{mq} to estimate T_e. With the help of the voltage-type flux linkage observer, ψ_d, ψ_q can be calculated through the coordinate transformation. However, the stator magnetizing current i_{md} and i_{mq} cannot be measured or calculated directly. Traditionally, the T_e is often estimated by the stator current i_d and i_q, as shown in equation(3):

$$\begin{aligned} T_e &= \frac{3}{2}P_n\left(\boldsymbol{\psi}_s \otimes \boldsymbol{i}_s\right) \\ &= \frac{3}{2}P_n\left(\psi_d i_q - \psi_q i_d\right) \end{aligned} \tag{3}$$

When the T_e is estimated by stator current, the estimation error of T_e can be expressed as:

$$\begin{aligned} \Delta T_e &= \frac{3}{2}P_n\left(\psi_d\left(i_q - i_{mq}\right) - \psi_q\left(i_d - i_{md}\right)\right) \\ &= \frac{3}{2}P_n\left(\psi_d i_{fq} - \psi_q i_{fd}\right) \end{aligned} \tag{4}$$

As shown in equation(4), when using stator current i_d and i_q to estimate torque, the current deviation caused by iron loss leads to an estimation error. In order to improve the estimation accuracy, it is necessary to obtain the stator magnetizing current i_{md} and i_{mq}.

Equation(1) shows the parameter relationship under the PMSM model considering iron loss. The third equation of Equation(1) shows that stator magnetizing current i_{md} and i_{mq} can be expressed by iron loss resistance R_f and stator current i_d and i_q. In other words, if the R_f can be estimated, then i_{md} and i_{mq} can be estimated through equation(5). When the estimated iron loss resistance $\hat{R}_f$ converges to the actual R_f, the estimated stator magnetizing current i_{md_est} and i_{mq_est} is also equal to the actual i_{md} and i_{mq}.

$$\begin{cases} L_{md}\dfrac{di_{md\_est}}{dt} = \hat{R}_f\left(i_d - i_{md\_est}\right) + w_e L_q i_{mq\_est} \\ L_{mq}\dfrac{di_{mq\_est}}{dt} = \hat{R}_f\left(i_q - i_{mq\_est}\right) - w_e L_d i_{md} - w_e\psi_f \end{cases} \tag{5}$$

where the sign "∧" represents the estimated value; i_{md_est} and i_{mq_est} is estimated stator magnetizing current.

Therefore, if the iron loss resistance R_f can be estimated, the estimation of T_e can be expressed as:

$$T_e = \frac{3}{2}P_n\left(\psi_d i_{mq\_est} - \psi_q i_{md\_est}\right) \tag{6}$$

III. MRAS-BASED IRON LOSS RESISTANCE OBSERVER

In the above analysis, the stator magnetizing current i_{md} and i_{mq} can be estimated through iron loss resistance R_f. Model reference adaptive system (MRAS) has been widely used in parameter identification [22], [23]. Generally speaking, MRAS is constructed on two models: the reference model and the adaptive model. With the help of nonlinear stability theorems, such as Lyapunov's or Popov's stability methods, an adaptation law must be designed reasonably to ensure the overall stability of the observer [10]. Based on the mathematical model of the PMSM considering the iron loss resistance, a novel MRAS-based iron loss resistance observer is designed to estimate iron loss resistance and stator magnetizing current simultaneously.

A. DESIGN OF THE OBSERVER

Based on Fig. 1, the reference model is constructed as follows:

$$p\begin{bmatrix} i_d \\ i_q \\ i_{md} \\ i_{mq} \end{bmatrix} = \begin{bmatrix} -\dfrac{R_s+R_f}{L_{ld}} & 0 & \dfrac{R_f}{L_{ld}} & 0 \\ 0 & -\dfrac{R_s+R_f}{L_{lq}} & 0 & \dfrac{R_f}{L_{lq}} \\ \dfrac{R_f}{L_{md}} & 0 & -\dfrac{R_f}{L_{md}} & \dfrac{L_q\omega_e}{L_{md}} \\ 0 & \dfrac{R_f}{L_{mq}} & -\dfrac{L_d\omega_e}{L_{mq}} & -\dfrac{R_f}{L_{mq}} \end{bmatrix} \times \begin{bmatrix} i_d \\ i_q \\ i_{md} \\ i_{mq} \end{bmatrix} + \begin{bmatrix} \dfrac{1}{L_{ld}} & 0 \\ 0 & \dfrac{1}{L_{lq}} \\ 0 & 0 \\ 0 & 0 \end{bmatrix}\begin{bmatrix} u_d \\ u_q \end{bmatrix} + \begin{bmatrix} 0 \\ 0 \\ 0 \\ -\dfrac{\omega_e\psi_f}{L_{mq}} \end{bmatrix} \tag{7}$$

The output matrix is designed $\boldsymbol{C} = \left[\begin{smallmatrix} 1 & 0 & 0 & 0 \\ 0 & 1 & 0 & 0 \end{smallmatrix}\right]$, and the output of the reference model is:

$$\begin{bmatrix} i_d \\ i_q \end{bmatrix} = \begin{bmatrix} 1 & 0 & 0 & 0 \\ 0 & 1 & 0 & 0 \end{bmatrix}\begin{bmatrix} i_d \\ i_q \\ i_{md} \\ i_{mq} \end{bmatrix} \tag{8}$$

The state-space representation of the reference model is rewritten as:

$$\begin{cases} p\boldsymbol{x} = \boldsymbol{Ax} + \boldsymbol{Bu} + \boldsymbol{d} \\ \boldsymbol{y} = \boldsymbol{Cx} \end{cases} \tag{9}$$

For the purpose of estimating the iron loss resistance R_f, the rotor electrical angular velocity ω_e can be obtained by the encoder, and other parameters can be measured offline in advance. Take the R_f as a parameter to be estimated; the adaptive model mode is constructed as follows:

$$p\begin{bmatrix} \hat{i}_d \\ \hat{i}_q \\ \hat{i}_{md} \\ \hat{i}_{mq} \end{bmatrix} = \begin{bmatrix} -\dfrac{R_s+\hat{R}_f}{L_{ld}} & 0 & \dfrac{\hat{R}_f}{L_{ld}} & 0 \\ 0 & -\dfrac{R_s+\hat{R}_f}{L_{lq}} & 0 & \dfrac{\hat{R}_f}{L_{lq}} \\ \dfrac{\hat{R}_f}{L_{md}} & 0 & -\dfrac{\hat{R}_f}{L_{md}} & \dfrac{L_q\omega_e}{L_{md}} \\ 0 & \dfrac{\hat{R}_f}{L_{mq}} & -\dfrac{L_d\omega_e}{L_{mq}} & -\dfrac{\hat{R}_f}{L_{mq}} \end{bmatrix} \times \begin{bmatrix} \hat{i}_d \\ \hat{i}_q \\ \hat{i}_{md} \\ \hat{i}_{mq} \end{bmatrix} + \begin{bmatrix} \dfrac{1}{L_{ld}} & 0 \\ 0 & \dfrac{1}{L_{lq}} \\ 0 & 0 \\ 0 & 0 \end{bmatrix}\begin{bmatrix} u_d \\ u_q \end{bmatrix} + \begin{bmatrix} 0 \\ 0 \\ 0 \\ -\dfrac{\omega_e\psi_f}{L_{mq}} \end{bmatrix} \tag{10}$$

The output matrix $\boldsymbol{C}$ is the same as above, the output of the adaptive model is:

$$\begin{bmatrix}\hat{i}_d\\ \hat{i}_q\end{bmatrix}=\begin{bmatrix}1 & 0 & 0 & 0\\ 0 & 1 & 0 & 0\end{bmatrix}\begin{bmatrix}\hat{i}_d\\ \hat{i}_q\\ \hat{i}_{md}\\ \hat{i}_{mq}\end{bmatrix} \tag{11}$$

The state-space representation of the adaptive model is rewritten as:

$$\begin{cases}p\hat{\boldsymbol{x}}=\hat{A}\hat{\boldsymbol{x}}+\boldsymbol{Bu}+\boldsymbol{d}\\ \hat{\boldsymbol{y}}=\boldsymbol{C}\hat{\boldsymbol{x}}\end{cases} \tag{12}$$

The error between the reference model and the adaptive model can be expressed as:

$$\begin{aligned}p\boldsymbol{e}&=\boldsymbol{Ax}-\hat{A}\hat{\boldsymbol{x}}\\ &=\boldsymbol{A}\left(\boldsymbol{x}-\hat{\boldsymbol{x}}\right)+\left(\boldsymbol{A}-\hat{\boldsymbol{A}}\right)\hat{\boldsymbol{x}}\\ &=\boldsymbol{Ae}-\left(\hat{R}_f-R_f\right)\boldsymbol{J}\hat{\boldsymbol{x}}\end{aligned} \tag{13}$$

where the error matrix of the state variables $\boldsymbol{e}=\left[i_d-\hat{i}_d\ i_q-\hat{i}_q\ i_{md}-\hat{i}_{md}\ i_{mq}-\hat{i}_{mq}\right]^T$; and

$$\boldsymbol{J}=\begin{bmatrix}-\dfrac{1}{L_{ld}} & 0 & \dfrac{1}{L_{ld}} & 0\\ 0 & -\dfrac{1}{L_{ld}} & 0 & \dfrac{1}{L_{ld}}\\ \dfrac{1}{L_{md}} & 0 & -\dfrac{1}{L_{md}} & 0\\ 0 & \dfrac{1}{L_{mq}} & 0 & -\dfrac{1}{L_{mq}}\end{bmatrix}.$$

B. DESIGN OF ADAPTATION LAW

The stability of the designed observer must be guaranteed to ensure that the error between R_f and $\hat{R}_f$ will converge to zero. By designing a compensation matrix $\boldsymbol{D}$, the error state equation can be equivalent to a nonlinear feedback system.

$$\begin{cases}p\boldsymbol{e}=\boldsymbol{Ae}-\boldsymbol{w}\\ \boldsymbol{v}=\boldsymbol{De}\\ \boldsymbol{w}=\left(\hat{R}_f-R_f\right)\boldsymbol{J}\hat{\boldsymbol{x}}\end{cases} \tag{14}$$

Where v represents the output of the linear block, and w represents the output of the nonlinear time-varying block.

The equivalent nonlinear feedback system is shown in Fig. 2.

Popov's stability criterion is used to verify the stability of the adaptation mechanism. According to Popov's stability criterion, the equivalent nonlinear feedback system shown in Fig. 2 is stable only if the following two conditions are satisfied.

(1) The forward path transfer function $\boldsymbol{G}_{(s)}=\boldsymbol{D}\left(s\boldsymbol{I}-\boldsymbol{A}\right)^{-1}$ is positive definite.

(2) The nonlinear feedback satisfies the following Popov's integral inequality:

$$\int_0^{t_1}\boldsymbol{w}^{\mathrm{T}}\boldsymbol{v}dt\geqslant-\gamma_0^2 \tag{15}$$

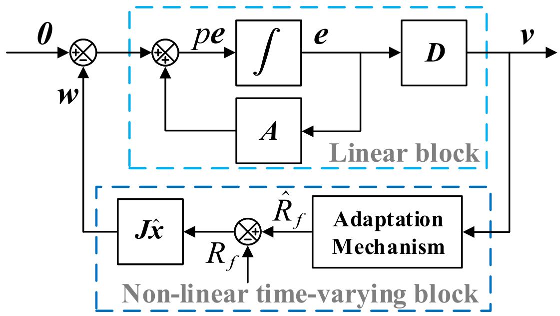

FIGURE 2. The equivalent non-linear feedback system.

Where $t_1\geqslant 0$ and γ_0 is an arbitrary positive constant.

The compensation matrix designed in this paper is $\boldsymbol{D}=\mathrm{diag}\left(\frac{L_{ld}}{L_{md}},\frac{L_{lq}}{L_{md}},1,\frac{L_{mq}}{L_{md}}\right)$, the output $\boldsymbol{v}$ is defined as:

$$\boldsymbol{v}=\begin{bmatrix}\dfrac{L_{ld}}{L_{md}} & 0 & 0 & 0\\ 0 & \dfrac{L_{lq}}{L_{md}} & 0 & 0\\ 0 & 0 & 1 & 0\\ 0 & 0 & 0 & \dfrac{L_{mq}}{L_{md}}\end{bmatrix}\begin{bmatrix}i_d-\hat{i}_d\\ i_q-\hat{i}_q\\ i_{md}-\hat{i}_{md}\\ i_{mq}-\hat{i}_{mq}\end{bmatrix} \tag{16}$$

For condition 1, the necessary and sufficient condition is that there are symmetric and positive definite matrices $\boldsymbol{P}$ and $\boldsymbol{Q}$, which satisfy the following conditions:

$$\begin{cases}\boldsymbol{PA}+\boldsymbol{A}^{\mathrm{T}}\boldsymbol{P}=-\boldsymbol{Q}\\ \boldsymbol{I}^{\mathrm{T}}\boldsymbol{P}=\boldsymbol{D}\end{cases} \tag{17}$$

Where $\boldsymbol{I}$ is the identity matrix, $\boldsymbol{I}=\mathrm{diag}\left(1,1,1,1\right)$.

Substituting the matrix $\boldsymbol{D}$ into the equation(17), the matrix $\boldsymbol{P}=\left(\frac{L_{ld}}{L_{md}},\frac{L_{lq}}{L_{md}},1,\frac{L_{mq}}{L_{md}}\right)$ and matrix

$$\boldsymbol{Q}=\frac{2}{L_{md}}\begin{bmatrix}R_s+R_f & 0 & -R_f & 0\\ 0 & R_s+R_f & 0 & -R_f\\ -R_f & 0 & R_f & 0\\ 0 & -R_f & 0 & R_f\end{bmatrix}.$$

The leading principal minors of matrix $\boldsymbol{Q}$ are obtained:

$$\begin{cases}Q_1=\dfrac{2\left(R_s+R_f\right)}{L_{md}}\\ Q_2=\dfrac{4\left(R_s+R_f\right)^2}{L_{md}^2}\\ Q_3=\dfrac{8R_sR_f\left(R_s+R_f\right)}{L_{md}^2}\\ Q_4=\dfrac{16R_s^2R_f^2}{L_{md}^4}\end{cases} \tag{18}$$

Where Q_i represents the determinant of the leading principal minor of order i.

It is obvious that diagonal matrix $\boldsymbol{P}$ is positive definite. The leading principal minors of symmetric matrix $\boldsymbol{Q}$ are all positive. It can be proved that the forward path transfer function $\boldsymbol{G}_{(s)}=\boldsymbol{D}\left(s\boldsymbol{I}-\boldsymbol{A}\right)^{-1}$ is positive definite.

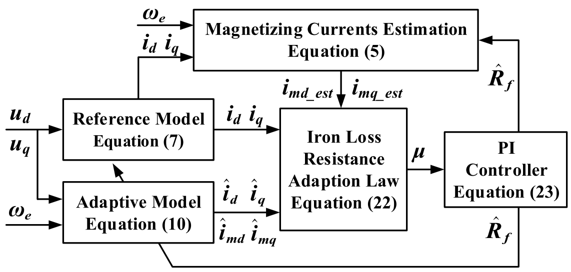

FIGURE 3. Block diagram of the iron loss resistance observer.

For condition 2, substituting matrix $\boldsymbol{v}$ and $\boldsymbol{w}$ into equation(15), the inequality becomes:

$$\int_0^{t_1} \left(\hat{R}_f - R_f\right)(\boldsymbol{J}\hat{\boldsymbol{x}})^{\mathrm{T}} \boldsymbol{De} \geqslant -\gamma_0^2 \tag{19}$$

From the inequality:

$$\int_0^{t_1} f(t)\frac{df(t)}{dt} = \frac{1}{2}\left(f^2(t_1) - f^2(0)\right) \geqslant -\frac{1}{2}f^2(0) \tag{20}$$

If we define:

$$\begin{cases} \hat{R}_f = R_f + f(t) \\ f(t) = \int_0^{t_1} (\boldsymbol{J}\hat{\boldsymbol{x}})^{\mathrm{T}} \boldsymbol{De}dt \end{cases} \tag{21}$$

With the aid of inequality(20) and equation(21), we can see that condition 2 is satisfied.

In steady-state, it is assumed that $\frac{dR_f}{dt} \approx 0$, because the change of the R_f in the time scale of the observer can be neglected. Differentiate $f(t)$ and substitute matrix $\boldsymbol{J}, \hat{\boldsymbol{x}}, \boldsymbol{D}$ and $\boldsymbol{e}$, $\frac{d\hat{R}_f}{dt}$ is expressed as:

$$\begin{aligned} \frac{d\hat{R}_f}{dt} &= \left(\left(\hat{i}_d - i_d\right) - \left(\hat{i}_{md} - i_{md}\right)\right)\left(\hat{i}_{md} - \hat{i}_d\right) \\ &\quad + \left(\left(\hat{i}_q - i_q\right) - \left(\hat{i}_{mq} - i_{mq}\right)\right)\left(\hat{i}_{mq} - \hat{i}_q\right) \end{aligned} \tag{22}$$

Combined with the PI controller and let $\frac{d\hat{R}_f}{dt} = \mu$, the estimated iron loss resistance $\hat{R}_f$ is:

$$\hat{R}_f = K_p\mu + K_i \int \mu dt \tag{23}$$

where K_p and K_i are the integral and proportional gains of PI controller, respectively.

In the operation of the observer, the stator magnetizing current i_{md} and i_{mq} are replaced by i_{md_est} and i_{mq_est}. The block diagram is shown in Fig. 3.

IV. SIMULATION VALIDATION

The proposed method is verified in MATLAB/Simulink with a torque-angle-based DTC strategy [24]. The control block diagram of the DTC with the designed observer is shown in Fig. 4.

The main parameters of the PMSM used in simulation are listed in Table 1.

The simulation step is $2\mu s$, the control cycle is $100\mu s$, and the bus voltage is 220V. The speed command n^* is 3000 rpm

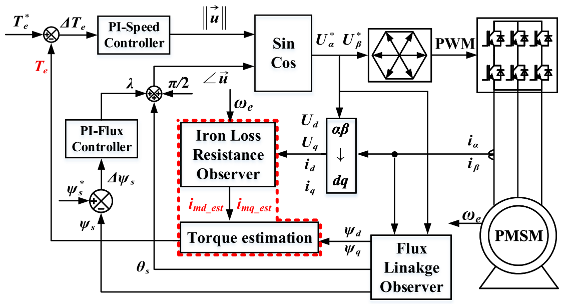

FIGURE 4. Control block diagram of the DTC with the designed observer.

TABLE 1. Main parameters of the PMSM.

Symbol	Parameters	Value and unit
P_n	Pole-pair numbers	4
L_{md}	Direct-axes magnetizing inductance	0.009 H
L_{mq}	Quadrature-axes magnetizing inductance	0.009 H
L_{ld}	Direct-axes leakage inductance	0.0015 H
L_{lq}	Quadrature-axes leakage inductance	0.0015 H
R_s	Stator resistance	0.87 Ω
R_f	Iron loss resistance	200 Ω
ψ_f	Rotor flux linkage	0.086 Wb
J	Rotor inertia	0.000159 kg · m^2
W_p	Rated power	1 kW
N_n	Rated speed	3000 rpm
T_n	Rated torque	3.2 N.m

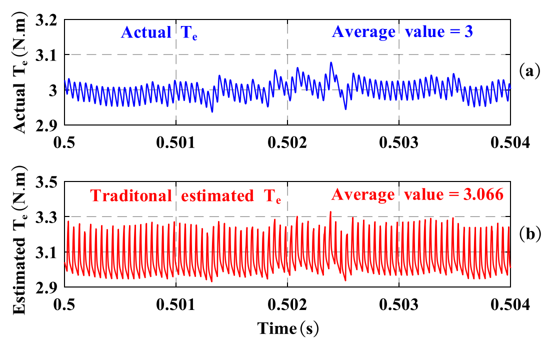

FIGURE 5. Torque estimation result by using stator current (speed = 3000 rpm, load = 3 N.m). (a) Actual value of the torque. (b) Estimated value of the torque.

in the test condition, and the stator flux linkage command ψ_s^* is 0.1 Wb.

When loading 3N.m, the estimated torque by using the stator current is 3.066 N.m. Compared to the actual 3 N.m load, the error of estimated accuracy is 2.2%. For convenience, this method is called the traditional method in this paper.

In the simulation, the R_f is set to 200 Ω. Fig. 6 shows the experimental result of the estimated iron loss resistance $\hat{R}_f$ under the proposed observer. The observer starts when it is unloaded, and after the observer converges, the loading experiment is carried out. The simulation result shows that the estimated $\hat{R}_f$ can converge to 197 Ω within 0.2 s. About 0.3 s, the estimation error is within 1%. The result shows that the designed observer has a good response speed and estimation accuracy.

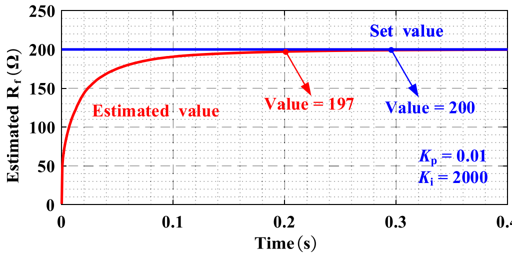

FIGURE 6. Estimation result of the iron loss resistance. (speed = 3000 rpm, load = 0 N.m).

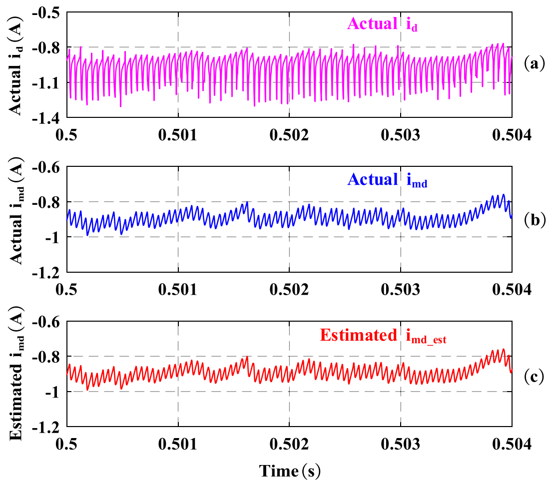

FIGURE 7. Simulation results of the d-axis current. (a) Actual stator current i_d. (b) Actual stator magnetizing current i_{md}. (c) Estimated stator magnetizing current i_{md_est}.

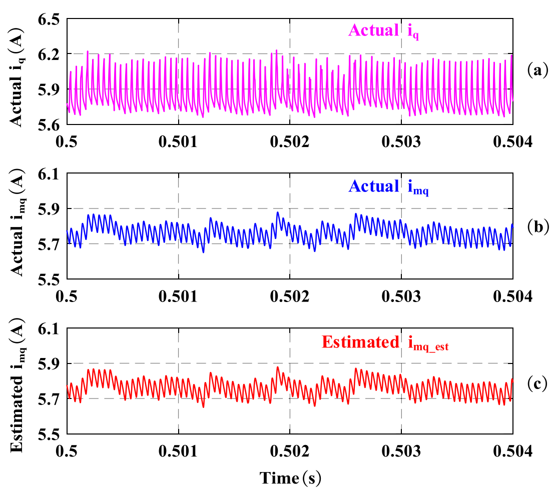

FIGURE 8. Simulation results of the q-axis current. (a) Actual stator current i_q. (b) Actual stator magnetizing current i_{mq}. (c) Estimated stator magnetizing current i_{mq_est}.

When the observer converges, the load is set to 3 N.m. Fig. 7 and Fig. 8 show the simulation results of d-axis and q-axis current. The results show that the estimated stator magnetizing current i_{md_est}, i_{mq_est} can match the actual stator magnetizing current i_{md}, i_{mq} well.

Fig. 9 shows the torque estimation result when the estimated stator magnetizing current i_{md_est} and i_{mq_est} is used.

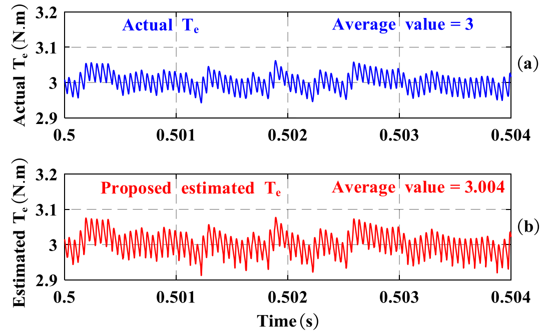

FIGURE 9. Torque estimation result by using magnetizing current (speed = 3000 rpm, load = 3 N.m). (a) Actual value of the torque. (b) Estimated value of the torque.

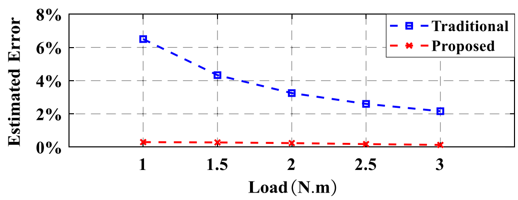

FIGURE 10. Simulation result of torque estimation accuracy under different load.

When the load is 3 N.m, the estimated torque is 3.004 N.m. Compared to the actual 3 N.m load, the error of estimated accuracy is only 0.13%. The error is reduced from 2.2% to 0.13%.

Fig. 10 shows the simulation result of torque estimation accuracy under different load. It can be seen that when using stator current to estimate the torque, the estimation error is within 6%. When using the estimated stator magnetizing current, the error is reduced to 1%. Based on these simulation results, it can be concluded that using magnetizing current to estimate torque can improve the estimation accuracy.

V. EXPERIMENTAL VERIFICATION

The experiment is carried out on the 1kW PMSM platform based on TMS320F28335. The switching frequency of the inverter is 10 kHz, and the cycle of the designed observer is $10\mu s$. Except that the R_f of the test motor is unknown, other parameters are the same as Table 1. By the way, the dead time is set to 4 μs in the experiment. In order to avoid the influence of the dead time effect on the experiment, the dead time compensation method proposed in [24] is adopted.

In the experiment, the stator flux command ψ_s^* is set to 0.1 Wb, and the torque estimation accuracy comparison experiment is carried out using the stator current and the estimated stator magnetizing current.

The estimation result of iron loss resistance varies with speed and load. Fig. 12 shows the estimated iron loss resistance $\hat{R}_f$ under the test condition. When the observer converges, the estimated value is 152.3 Ω.

Fig. 13 and Fig. 14 show the magnetizing current i_{md_est} and i_{mq_est} estimated by the observer and the actual stator current i_d and i_q of the motor.

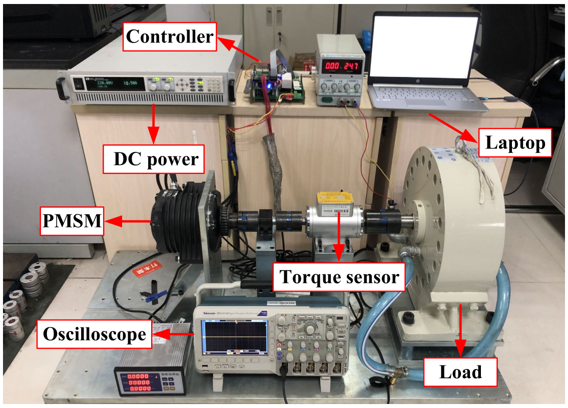

FIGURE 11. Platform of PMSM control system.

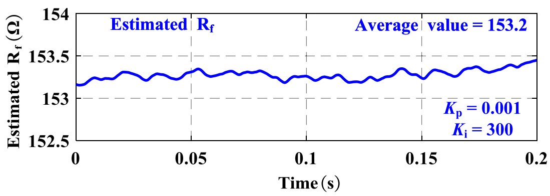

FIGURE 12. Estimation result of the iron loss resistance (speed = 3000 rpm, load = 3 N.m).

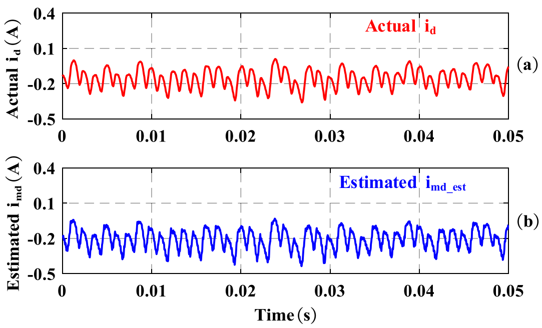

FIGURE 13. Experimental results of the d-axis current. (a) Actual stator current i_d. (b) Estimated stator magnetizing current i_{md_est}.

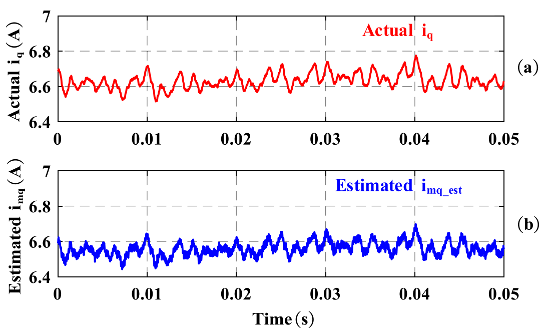

FIGURE 14. Experimental results of the q-axis current. (a) Actual stator current i_q. (b) Estimated stator magnetizing current i_{mq_est}.

Fig. 15 shows the torque estimation results using the stator current and the estimated stator magnetizing current. When the load is 3N.m, the estimated torque are 3.075 N.m and 3.013 N.m respectively. Compared to the actual 3 N.m load, the error of estimated accuracy is only 0.13%. The estimation error of electromagnetic torque is reduced from 2.5% to 0.13%.

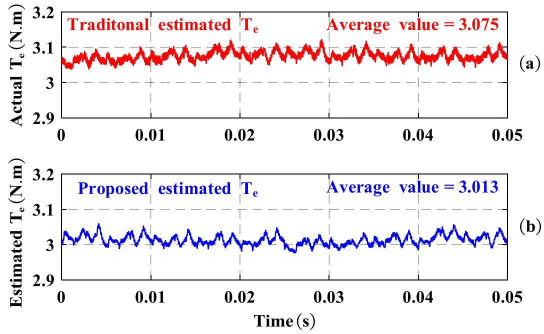

FIGURE 15. Experimental result of torque estimation. (speed = 3000 rpm, load = 3 N.m). (a) Torque estimation result by using stator current. (b) Torque estimation result by using estimated stator magnetizing current.

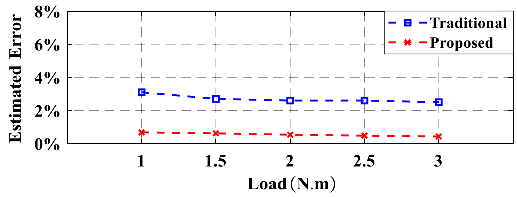

FIGURE 16. Experimental result of torque estimation accuracy under different load.

Fig. 16 shows the experimental result of torque estimation accuracy under different load. It can be seen that the torque estimation error of the two methods all less than 4%, but the method proposed in this paper has better accuracy.

VI. CONCLUSION

In this paper, a direct torque control of permanent magnet synchronous motor with high torque estimation accuracy is proposed. Firstly, based on the PMSM mathematical model considering the iron loss resistance, the torque estimation error caused by the iron loss resistance is analyzed. Then, a novel iron loss resistance observer based on MRAS is designed to estimate iron loss resistance and stator magnetizing current simultaneously. Popov's hyperstability theory guarantees the stability of the designed observer. Finally, both simulation and experiment prove the availability of the proposed method.

REFERENCES

[1] J. Hang, H. Wu, S. Ding, W. Hua, and Q. Wang, "A DC-flux-injection method for fault diagnosis of high-resistance connection in direct-torque-controlled PMSM drive system," *IEEE Trans. Power Electron.*, vol. 35, no. 3, pp. 3029–3042, Mar. 2020.

[2] W. Wang, H. Ma, X. Qiu, and J. Yang, "A calculation method for the on-load cogging torque of permanent magnet synchronous machine," *IEEE Access*, vol. 7, pp. 106316–106326, 2019.

[3] Y. Shim, S. K. Kauh, and K.-P. Ha, "Evaluation of idle stability through *in-situ* torque measurement in automatic transmission vehicles," *Int. J. Automot. Technol.*, vol. 12, no. 3, pp. 315–320, Jun. 2011.

[4] X. Wang, Z. Wang, Z. Xu, M. Cheng, and Y. Hu, "Optimization of torque tracking performance for direct-torque-controlled PMSM drives with composite torque regulator," *IEEE Trans. Ind. Electron.*, vol. 67, no. 12, pp. 10095–10108, Dec. 2020.

[5] C. Xia, S. Li, Y. Shi, X. Zhang, Z. Sun, and W. Yin, "A non-smooth composite control approach for direct torque control of permanent magnet synchronous machines," *IEEE Access*, vol. 7, pp. 45313–45321, 2019.

[6] Z. Wang, J. Chen, M. Cheng, and K. T. Chau, "Field-oriented control and direct torque control for paralleled VSIs fed PMSM drives with variable switching frequencies," *IEEE Trans. Power Electron.*, vol. 31, no. 3, pp. 2417–2428, Mar. 2016.

[7] L. Zhong, M. F. Rahman, W. Y. Hu, and K. W. Lim, "Analysis of direct torque control in permanent magnet synchronous motor drives," *IEEE Trans. Power Electron.*, vol. 12, no. 3, pp. 528–536, May 1997.

[8] F. Niu, X. Huang, L. Ge, J. Zhang, L. Wu, Y. Wang, and K. Li, "A simple and practical duty cycle modulated direct torque control for permanent magnet synchronous motors," *IEEE Trans. Power Electron.*, vol. 34, no. 2, pp. 1572–1579, Feb. 2019.

[9] F. Niu, B. Wang, A. S. Babel, K. Li, and E. G. Strangas, "Comparative evaluation of direct torque control strategies for permanent magnet synchronous machines," *IEEE Trans. Power Electron.*, vol. 31, no. 2, pp. 1408–1424, Feb. 2016.

[10] M. H. Holakooie, M. Ojaghi, and A. Taheri, "Direct torque control of six-phase induction motor with a novel MRAS-based stator resistance estimator," *IEEE Trans. Ind. Electron.*, vol. 65, no. 10, pp. 7685–7696, Oct. 2018.

[11] J. Hu and B. Wu, "New integration algorithms for estimating motor flux over a wide speed range," *IEEE Trans. Power Electron.*, vol. 13, no. 5, pp. 969–977, Sep. 1998.

[12] H. Saberi, M. Sabahi, M. B. B. Sharifian, and M. Feyzi, "Improved sensorless direct torque control method using adaptive flux observer," *IET Power Electron.*, vol. 7, no. 7, pp. 1675–1684, Jul. 2014.

[13] X. Lin, W. Huang, W. Jiang, Y. Zhao, and S. Zhu, "A stator flux observer with phase self-tuning for direct torque control of permanent magnet synchronous motor," *IEEE Trans. Power Electron.*, vol. 35, no. 6, pp. 6140–6152, Jun. 2020.

[14] J. Shi and S. Li, "Analysis and compensation control of dead-time effect on space vector PWM," *J. Power Electron.*, vol. 15, no. 2, pp. 431–442, Mar. 2015.

[15] A. Aimad, K. Madjid, and S. Mekhilef, "Robust sensorless sliding mode flux observer for DTC-SVM-based drive with inverter nonlinearity compensation," *J. Power Electron.*, vol. 14, no. 1, pp. 125–134, Jan. 2014.

[16] T. Qiu, X. Wen, and F. Zhao, "Adaptive-linear-neuron-based dead-time effects compensation scheme for PMSM drives," *IEEE Trans. Power Electron.*, vol. 31, no. 3, pp. 2530–2538, Mar. 2016.

[17] S. Yamamoto, H. Hirahara, A. Tanaka, T. Ara, and K. Matsuse, "Universal sensorless vector control of induction and permanent-magnet synchronous motors considering equivalent iron loss resistance," *IEEE Trans. Ind. Appl.*, vol. 51, no. 2, pp. 1259–1267, Mar. 2015.

[18] J. Hang, H. Wu, S. Ding, Y. Huang, and W. Hua, "Improved loss minimization control for IPMSM using equivalent conversion method," *IEEE Trans. Power Electron.*, vol. 36, no. 2, pp. 1931–1940, Feb. 2021.

[19] N. Urasaki, T. Senjyu, and K. Uezato, "Relationship of parallel model and series model for permanent magnet synchronous motors taking iron loss into account," *IEEE Trans. Energy Convers.*, vol. 19, no. 2, pp. 265–270, Jun. 2004.

[20] C. Cavallaro, A. O. D. Tommaso, R. Miceli, A. Raciti, G. R. Galluzzo, and M. Trapanese, "Efficiency enhancement of permanent-magnet synchronous motor drives by online loss minimization approaches," *IEEE Trans. Ind. Electron.*, vol. 52, no. 4, pp. 1153–1160, Aug. 2005.

[21] N. Urasaki, T. Senjyu, and K. Uezato, "A novel calculation method for iron loss resistance suitable in modeling permanent-magnet synchronous motors," *IEEE Trans. Energy Convers.*, vol. 18, no. 1, pp. 41–47, Mar. 2003.

[22] L.-Y. Lu, N. F. Avila, C.-C. Chu, and T.-W. Yeh, "Model reference adaptive back-electromotive-force estimators for sensorless control of grid-connected DFIGs," *IEEE Trans. Ind. Appl.*, vol. 54, no. 2, pp. 1701–1711, Mar. 2018.

[23] S. Mohan Krishna and J. L. Febin Daya, "MRAS speed estimator with fuzzy and PI stator resistance adaptation for sensorless induction motor drives using RT-lab," *Perspect. Sci.*, vol. 8, pp. 121–126, Sep. 2016.

[24] X. Qiu, W. Huang, and F. Bu, "Torque-Angle-Based direct torque control for interior permanent-magnet synchronous motor drivers in electric vehicles," *J. Power Electron.*, vol. 13, no. 6, pp. 964–974, Nov. 2013.

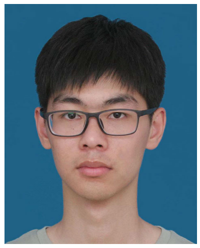

ZHEN JIN was born in Lianyungang, Jiangsu, China, in 1997. He received the B.S. degree in electrical engineering from Jiangsu University of Science and Technology, in 2019. He is currently pursuing the degree with the Electrical Engineering Department, School of Electrical and Automation Engineering, Nanjing Normal University. His research interest includes high-performance control strategies of PMSM.

JIANFEI YANG was born in Nantong, Jiangsu, China, in 1982. He received the B.S. and Ph.D. degrees in electrical engineering from Nanjing University of Aeronautics and Astronautics, in 2005 and 2011, respectively. Since 2017, he has been an Associate Professor with the Electrical Engineering Department, School of Electrical and Automation Engineering, Nanjing Normal University. His research interests include high-performance control methods of the permanent magnet synchronous motor and 3D printing (rapid prototyping technology).

XIN QIU was born in Huai'an, Jiangsu, China, in 1985. He received the B.S., M.S., and Ph.D. degrees in electrical engineering from Nanjing University of Aeronautics and Astronautics, in 2007, 2010, and 2014, respectively. Since 2014, he has been an Associate Professor with the Electrical Engineering Department, School of Electrical and Automation Engineering, Nanjing Normal University. His research interests include the design of permanent magnet motor and high performance control, 3D printing control systems, and electric vehicle electric drive systems.

HAORUI GE (Graduate Student Member, IEEE) was born in Huai'an, Jiangsu, China, in 1997. He received the B.S. degree in electrical engineering from Nanjing Normal University, in 2019, where he is currently pursuing the M.S. degree with the Electrical Engineering Department, School of Electrical and Automation Engineering. His research interests include electromagnetic design and noise optimization of PMSM.

CHENGUANG BAI was born in Nantong, Jiangsu, China. He received the B.S. degree in electrical engineering from Yancheng Institute of Technology, in 2018. He is currently pursuing the M.S. degree with the Electrical Engineering Department, School of Electrical and Automation Engineering, Nanjing Normal University. His research interest includes active disturbance rejection control of PMSM drives.